



INFLUENCE OF INFLOW TURBULENCE ON AEROACOUSTIC NOISE OF LOW SPEED AXIAL FANS WITH SKEWED AND UNSKEWED BLADES

Florian ZENGER, Marcus BECHER, Stefan BECKER

*Friedrich-Alexander University of Erlangen-Nuremberg,
Institute of Process Machinery and Systems Engineering,
Fluid System Dynamics and Aeroacoustics,
Cauerstr. 4, 91058 Erlangen, Germany*

SUMMARY

An experimental investigation was carried out on the effect of increased inflow turbulence on the aeroacoustic noise radiation of low speed axial fans with backward-, forward- and unskewed fan blades. Therefore, three different fans with one common operating point were designed with a 2D blade element method. Different grids were mounted to the inlet of the fans to increase the inflow turbulence intensity. Without and with a fine grid, the forward skewed fan shows the lowest SPL, however with a coarse grid, the backward skewed fan shows the lowest SPL. This is mainly, because tonal and low-frequency broadband components are elevated most noticeable for the forward skewed fan.

INTRODUCTION

The aeroacoustic noise radiation has become a key parameter to be taken into account during the design and development of low speed axial fans. On the one hand, noise radiation is dependent on the fan's design and operating point, on the other hand it is highly influenced by the boundary conditions under its operation, like e.g. inflow turbulence intensity. Design strategies for a reduced noise emission mostly include the use of sweep and dihedral.

Sweep and dihedral are used to describe a shifting of the airfoil sections in axial and/or tangential direction, as described by Gallimore [1] and Beiler [2]. Blade sweep is defined by a sweep angle λ which is the angle between the mean flow and the leading edge (alternatively also trailing edge or stacking line) of the blade. Positive values for λ conventionally describe a forward swept blade (sweep in circumferential direction) and negative values a backward swept blade (sweep against circumferential direction). The blade dihedral angle ν describes a shifting of the blade section normal to the section chord line. A skewed blade features both sweep and dihedral. Modern design

strategies mostly incorporate forward skewed fan blades as they are known to reduce pressure losses in the hub and tip regions [3], [4] and improve the acoustic behavior [5], [4].

There are several reasons, why skewed fans have a lower noise radiation than unskewed fans. Firstly, as described in [4], blade skew reduces tonal noise emitted by axial fans. This is mainly due to a reduction of unsteady blade forces as each section of the fan blades interacts with the inflow at a different instant. A study from Sturm [6] showed that tonal components at the blade passing frequency can be reduced by homogenizing the inflow.

Secondly, broadband noise is influenced by skewed blades. Depending on the blade skew (forward or backward), the turbulent boundary layer thickness is reduced (forward skewed fan blades) or increased (backward skewed fan blades) [5]. If a backward sweep is applied, the boundary layer fluid will move further in radial direction as there is a longer possible flow path before reaching the trailing edge – the opposite applies to forward sweep. As a consequence of this, the boundary layer thickness of backward skewed fans is expected to be thicker. As broadband noise is amongst others influenced by pressure fluctuations on the blade surface due to the turbulent boundary layer, this mechanism is considered to be more dominant for backward skewed fans. Kerschen and Envia [7] investigated the influence of the interaction of high frequency inflow turbulence with the leading edge of a finite span swept airfoil. They concluded that a blade sweep can be beneficial due to destructive interferences of acoustic pressure generated on adjacent spots. According to Wright [5], a backward swept blade is considered to reduce the noise due to interaction of turbulent inflow with the fans blades' leading edge more efficiently than forward swept blades. However, no further explanation is given for this. A study of the effect of different inflow distortions on the sound emission of an unskewed fan, including increased turbulence intensity, was done by Schneider [8]. He states that the overall sound pressure level can be profoundly influenced by increased inflow turbulence.

So far, the mechanisms of the interaction between increased inflow turbulence and skewed fan blades are not fully understood. Thus the main object of this work is to investigate the influence of both inflow turbulence and blade skew on the aeroacoustic noise radiation of axial fans.

FAN DESIGN

Three fans were designed using a 2D element blade method [9], [10]:

- N1UG: unskewed fan blades
- N1RG45: backward skewed fan blades
- N1VG45: forward skewed fan blades

The chosen design parameters at the operating point for all fans are listed below. The fans have the same overall design parameters except the sweep angle λ which varies for every fan. A free vortex design was used for blade circulation distribution.

Table 1: Fan design parameters at design point

	N1UG	N1RG45	N1VG45
flow rate coefficient Φ	0.19		
pressure coefficient ψ_t	0.2		
number of blades z	9		
rotational speed n in rpm	1500		
fan diameter D in mm	495		
hub diameter D_{hub} in mm	248		

tip clearance s in mm	2.5		
blade airfoil	NACA 4510		
sweep angle λ (constant) in deg.	0	-45	+45
dihedral angle ν in deg.	0		

With the flow rate coefficient Φ :

$$\Phi = 4 \frac{\dot{V}}{\pi^2 D^3 n} \quad (1)$$

And the pressure coefficient ψ_t :

$$\psi_t = 2 \frac{\Delta p_t}{\rho (D \pi n)^2} \quad (2)$$

Here, \dot{V} is the volume flow rate, ρ the air density and Δp_t the total pressure difference, calculated according to:

$$\Delta p_t = \Delta p_{static} + \frac{\rho}{2} \left(\frac{4\dot{V}}{\pi D_{duct}^2} \right)^2 \quad (3)$$

The static pressure difference Δp_{static} is the pressure difference between the ambient pressure and the pressure inside the test chamber (on the fan's suction side). The second part in equation (3) is the dynamic pressure, calculated via volume flow rate and the mean velocity in the open duct section, with the duct diameter $D_{duct} = 500$ mm.

The 2D element blade method is based on the assumption that the flow around a fan blade is not influenced by the adjacent fan blades. The governing equation for designing low solidity blade cascades is:

$$\frac{l}{t} = \frac{2 \cdot \tilde{\epsilon}}{c_L \cdot w_\infty \cdot u \cdot \left(1 + \frac{\epsilon}{\tan \beta_\infty} \right)} \quad (4)$$

In equation (4), l is the blade chord length, t the blade spacing, $\tilde{\epsilon}$ the specific shaft work, c_L the lift coefficient, w_∞ the average flow velocity in the rotating frame of reference, u the circumferential velocity, ϵ the drag to lift ratio and β_∞ the angle between w_∞ and the fan blade. It incorporates the solidity $\frac{l}{t}$ (left hand side of equation (4)) as well as parameters of the ventilator operating point and the selected airfoil (right hand side of equation (4)). To use equation (4), the fan blade is divided into sections of equal area. Then for each section, the airfoil chord length is calculated at the mean diameter of the inner and outer diameter of each section according to equation (4). The first and last diameter for these calculations is always hub- and tip-diameter. Each blade segment is then shifted according to the corresponding diameter, angle of attack, sweep and dihedral.

When applying sweep to the fan blade, the lift of the airfoil is reduced by a theoretical factor of $\cos \lambda$ [2]. Beiler [2] found a factor of $\cos \lambda^{0.62}$ to be in better agreement with actual test rig measurements. Thus this factor was used during the design process. XFOIL [11] was used to obtain lift- and drag coefficients for each blade section.



Figure 1: Unskewed fan NIUG (left), backward skewed fan NIRG45 (middle) and forward skewed fan NIVG45 (right)
– rotational direction: clockwise

EXPERIMENTAL SETUP

Fan characteristic curves were measured at a standardized inlet test chamber according to ISO 5801 [12]. The fans were installed in a short duct with the length of three times the duct diameter. Volume flow, static pressure difference (ambient to chamber), torque, rotational speed, ambient pressure and temperature are captured throughout the period of test for each test point. The test chamber was built as a semi-anechoic chamber to enable aeroacoustic measurements.

To increase the inflow turbulence intensity, three different grids were mounted to the inlet section of the duct:

- grid 20: 20 mm clearance, bar width $d_b = 4$ mm (mesh size $M = 24$ mm)
- grid 60: 60 mm clearance, bar width $d_b = 12$ mm (mesh size $M = 72$ mm)
- grid 80: 80 mm clearance, bar width $d_b = 16$ mm (mesh size $M = 96$ mm)

The grid solidity α is identical for all three grids:

$$\alpha = 2 \frac{d_b}{M} - \frac{d_b^2}{M^2} = 0.31 \quad (5)$$

The grids were mounted at a distance of 190 mm to the fan hub (see Figure 4).



Figure 2: Turbulence grids - grid 20 (left) and grid 80 (right)

Sound pressure field

The sound pressure field was measured with seven 1/2'' free field microphones which were placed at a distance of 1 m to the inlet duct at angular positions of -90, -60, -30, 0, +30, +60 and +90 degrees from the fan's rotational axis in a horizontal plane at the same height as the rotational axis (see Figure 3). The sound power level L_W was calculated from the measurement data of each microphone [13]:

$$L_W = \overline{L_P} + 10 \log \left(\frac{A}{A_0} \right) \text{ dB} \quad (6)$$

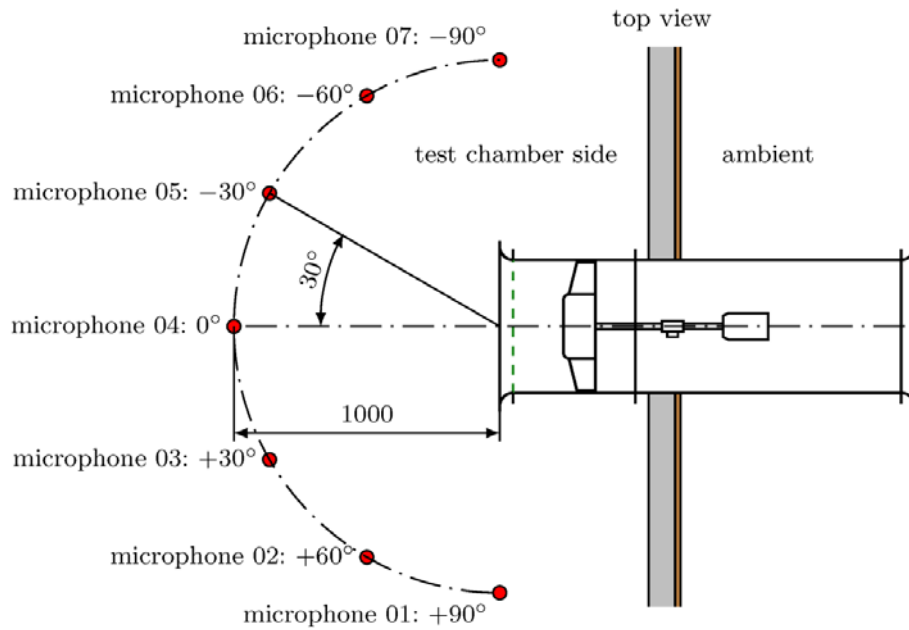


Figure 3: Schematic representation of microphone positions

Turbulence parameters

A Laser Doppler Anemometry (LDA) system was used to measure the axial velocity c_m at the ducted flow field on the fan's suction side. To obtain the required optical access to the flow field inside the duct, a small part of the duct was replaced with a glass screen. The LDA probe was attached to a traversing system which enabled the probe to be moved in radial direction. DANTEC BSA Flow software was used for signal processing and data evaluation.

During the velocity measurements, the fan was replaced with a hub dummy which had the same hub geometry but no fan blades. The auxiliary fan of the test chamber was used to generate the desired volume flow rate. Flow parameters were measured at the position of the leading edge of the fan blades. Four configurations – without grid and with installed grid 20, 60 and 80 – were investigated. In total, 12 measurement points were distributed radially from the hub to the duct wall. A schematic representation of the experimental setup is given in Figure 4.

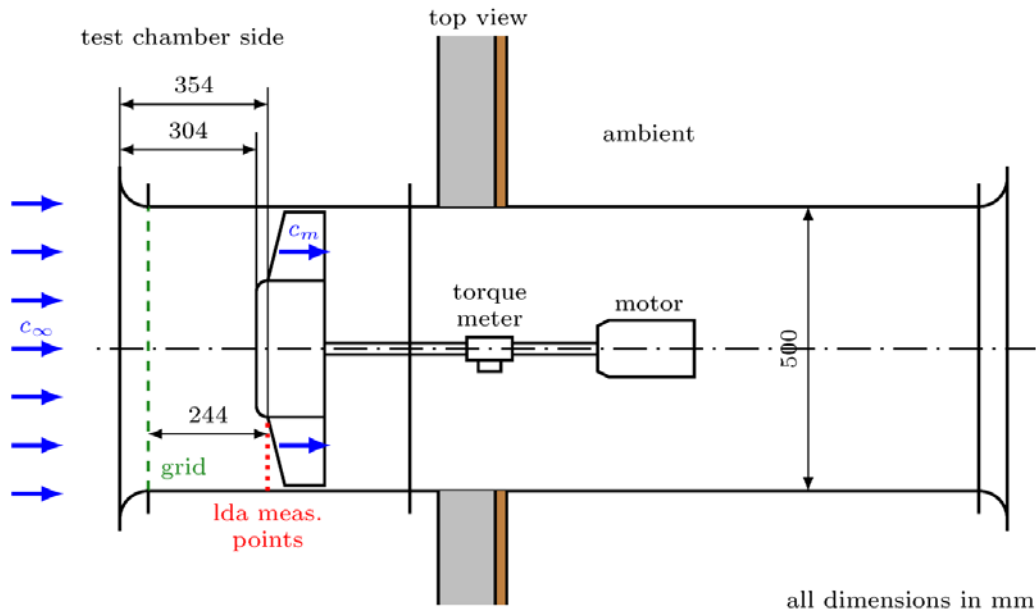


Figure 4: Schematic representation of grid position and LDA measurement points

RESULTS

This section includes the results for the fan characteristic curves, the measured radial distribution of the turbulence intensity and sound power spectra.

Fan characteristic curves

Figure 5 shows the fan characteristic curve for all no-grid configurations. The flow rate coefficient Φ and the pressure coefficient ψ_t are calculated according to equation (1) and (2). The efficiency is defined as

$$\eta_t = \frac{\dot{V} \Delta p_t}{2 \pi n M} \quad (7)$$

Here M is the measured torque by the torque meter (see Figure 4).

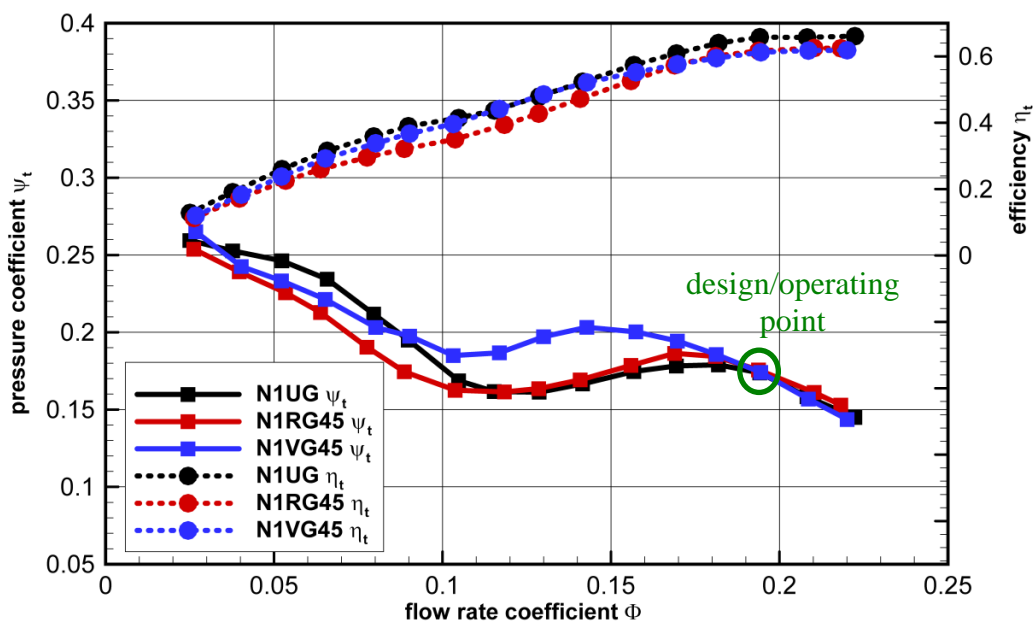


Figure 5: Fan characteristic curves (no grid-configurations)

The pressure coefficient curves of all three fans show similar values at the design flow rate coefficient of $\Phi = 0.19$. The values are 5-10 % less than the design pressure coefficient. As the difference is the same for all three fans, it can be assumed that this is due to additional losses which are neglected during the design procedure. One possible reason for such losses can be the hub geometry, which is not aerodynamically optimized. Another reason can be losses due to the interaction of the fan exit flow field with the drive motor.

The fan characteristic curves show the expected extension of the stall-free operational range for the forward skewed fan N1VG45 at flow rates below the design point, described e.g. in [14] and [15]. Only little discrepancy can be observed for the efficiency curve for the three fans. At the design point, the unskewed fan N1UG has the highest total efficiency while the efficiency of both skewed fans is 3 % less at the design point.

All further investigations are carried out at the design flow rate of $\Phi = 0.19$.

Grid-induced turbulence

The radial distribution of the turbulence intensity Tu without grid and with the three installed grids is shown in Figure 6. Downstream of the grids, the turbulence can be assumed to be isotropic [16]. Thus, the turbulence intensity can be calculated from the velocity fluctuations c'_m in axial direction, scaled by either the local velocity or a reference velocity. In this case, the measured mean velocity through the open area between hub and duct was chosen as reference velocity.

$$c_{ref} = \frac{1}{r_a - r_i} \int_{r_i}^{r_a} \overline{c_m}(r) dr \quad (8)$$

$$Tu = \frac{\sqrt{\overline{c_m'^2}}}{c_{ref}} \quad (9)$$

The bar over the velocity components denotes sample averaging.

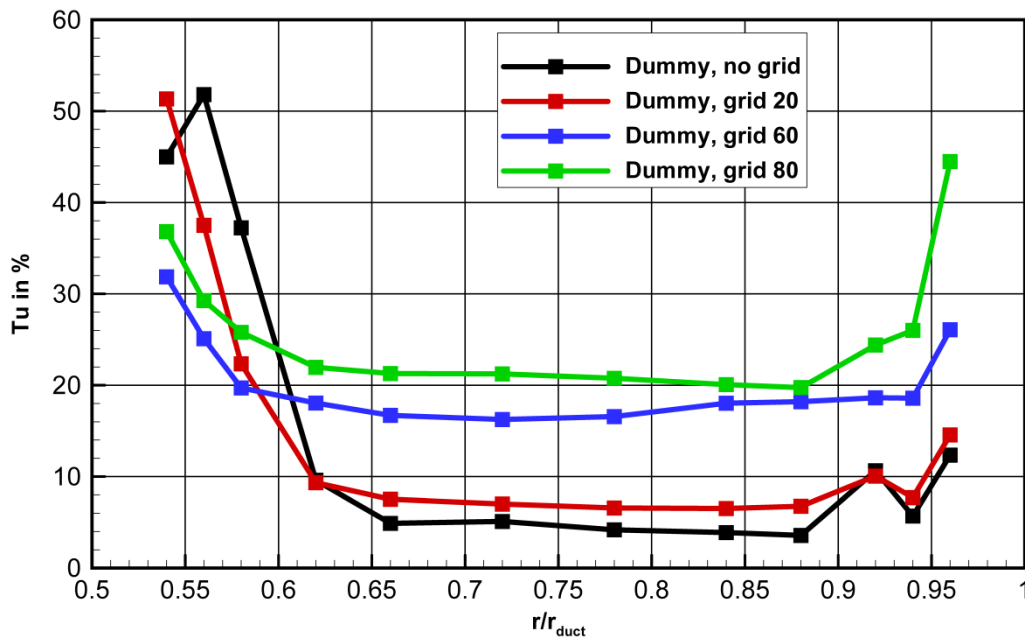


Figure 6: Radial distribution of turbulence intensity at $\Phi = 0.19$ with installed hub dummy

For values of $r/r_{duct} = 0.5 \dots 0.65$, a clear influence of the hub on the turbulence intensity can be seen. The turbulence intensity reaches values of nearly up to 55 % in this region. This confirms the assumption of additional pressure losses in the hub region, as described above. Towards the duct wall, values for Tu tend to increase again for measurements points above $r/r_{duct} = 0.95$. In between these two regions, the turbulence intensity is rather constant, reaching different mean values for each configuration:

- no grid: Tu \approx 5 %
- grid 20: Tu \approx 7 %
- grid 60: Tu \approx 17 %
- grid 80: Tu \approx 20 %

Based on these results, it can be stated that the inflow turbulence can be influenced over a wide range from Tu \approx 5 % to Tu \approx 20 %. The impact of increased inflow turbulence on the aeroacoustic noise radiation of the three different fans will be described in the next section.

Comparison of overall sound power level and sound power spectra

The following diagrams show the sound power level for each fan without grid and with grid 20, 60 and 80. In the following diagrams and tables, the overall sound power level L_W is calculated only in the displayed frequency range from 0.1 to 10 kHz. This is mainly to avoid low-frequency influence of room acoustics parameters of the semi-anechoic chamber.

Table 2 shows the overall sound power level L_W for all measured configurations. At undistorted inflow (no grid), the forward skewed fan N1VG45 shows the least overall sound power level. Hence, the beneficial effect of forward skew can be confirmed with this work. The backward skewed fan N1RG45 and the unskewed fan N1UG both show higher sound power levels with fan N1UG showing the highest value of the three fans of 84.6 dB. The same tendency applies under the influence of a moderate increase of inflow turbulence (grid 20). The rise in L_W is least distinctive for the fan N1VG45 (+0.6 dB) here. The impact of high inflow turbulence intensity (grid 60 and grid 80) is most significant for the forward skewed fan N1VG45 with a rise of +6.8 dB (grid 60) and +9.4 dB (grid 80) compared to the no grid-configuration while the unskewed fan N1UG only sees a rise of 5.7 dB (grid 60) and 6.7 dB (grid 80) and the backward fan N1RG45 3.9 dB (grid 60) and 5.4 dB (grid 80), see also Table 2. Explanations for this phenomenon will be given at the description of the acoustic spectra below.

Table 2: Overall sound power level L_W for all configurations, in brackets: L_W difference to no grid-configuration

	N1UG	N1RG45	N1VG45
no grid	84.6 dB	83 dB	81.2 dB
grid 20	87.2 dB (+ 2.6 dB)	84 dB (+ 1 dB)	81.8 dB (+ 0.6 dB)
grid 60	90.3 dB (+ 5.7 dB)	86.9 dB (+ 3.9 dB)	88 dB (+ 6.8 dB)
grid 80	91.3 dB (+ 6.7 dB)	88.4 dB (+ 5.4 dB)	90.6 dB (+ 9.4 dB)

The influence of increased inflow turbulence on the sound power level can be seen on both tonal and broadband components of the spectrum at frequencies below 2 kHz. The broadband noise above 2 kHz is hardly influenced by increased turbulence intensity.

One effect of increased inflow turbulence which can be observed for all fans is the elevation of tonal peaks at the blade passing frequency at 225 Hz and its harmonics. The fan N1VG45 shows the greatest elevation in tonal components while the fan N1RG45 shows the lowest elevation. As described above, tonal components are a result of unsteady blade forces, caused e.g. by the

interaction of turbulent structures at the inflow with the fan blades. It is assumed that this interaction is more gradually for backward skewed fan blades than for forward or unskewed fan blades, as turbulent structures have the possibility to migrate towards the blade tip and thereby dissipate energy. This is supported by the backward skewed geometry of the fan which tends to enable outward migration of fluid while this effect is suppressed especially for forward skewed fans. As a consequence of this, the forward skewed fan N1VG45 shows the highest elevation of tonal components of all three fans.

Another effect of increased inflow turbulence is an elevation of non-tonal low frequency components. This can be observed for all fans. While the elevation is similar for all fans for the grid 20-configuration, the elevation for the grid 60- and grid 80-configuration is higher for fan N1VG45 than for the other fans. It is assumed that this has the similar reason as stated above. Turbulent structures tend to interact less vigorously with backward skewed blades than with forward skewed blades. Another beneficial effect of backward skewed fans is the fact that the more intensified crossflow (radial flow) interacts with turbulent structures thus influencing their shape. The flow induced variations of angle of attack due to turbulent structures can thereby be reduced which leads to a lower noise radiation in the low frequency domain.

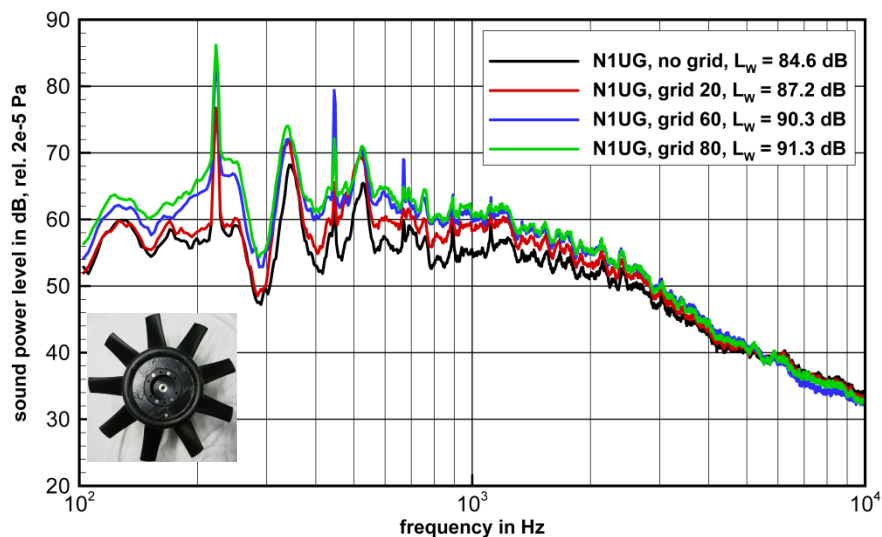


Figure 7: Sound power level spectra, fan N1UG for $\Phi = 0.19$ – configurations with and without grid

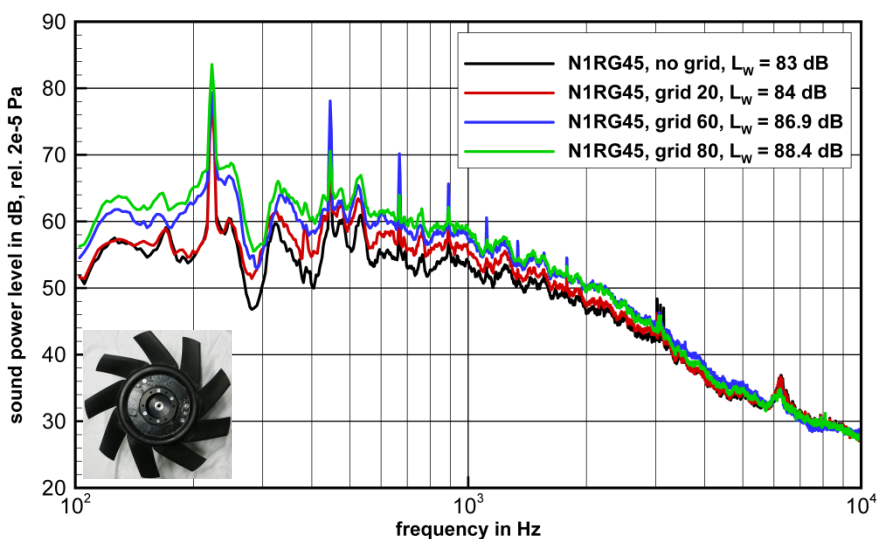


Figure 8: Sound power level spectra, fan N1RG45 for $\Phi = 0.19$ – configurations with and without grid

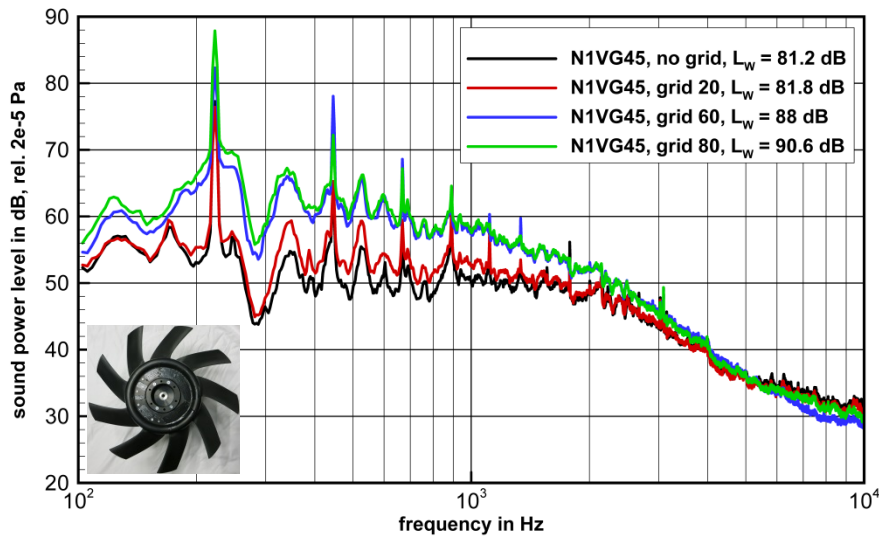


Figure 9: Sound power level spectra, fan N1VG45 for $\Phi = 0.19$ – configurations with and without grid

CONCLUSION

The effect of increased inflow turbulence on the aeroacoustic noise radiations of three different fans with different stacking strategies was investigated. All fans showed elevated tonal components at the blade passing frequency and its harmonics as well as elevated broadband components in the low frequency domain below 2 kHz. It was examined that for regular inflow conditions (no grid) and for a moderate rise of turbulence intensity (grid 20), the forward skewed fan N1VG45 shows the lowest sound power level and shows the least elevation in tonal and broadband components. This observation changes for high inflow turbulence intensities (grid 60 and grid 80). Here, the backward skewed fan N1RG45 shows the lowest overall sound pressure level with a difference of 0.4 dB (grid 60) and 2.9 dB (grid 80) to the unskewed fan N1UG and 1.1 dB (grid 60) and 2.2 dB (grid 80) to the forward skewed fan N1VG45. The fan N1VG45 shows the most noticeable elevation in both tonal and broadband components for high inflow turbulence intensities of all three fans. It is assumed that this is due to a changed interaction mechanism of the turbulent structures on the one hand with the leading edge of the fan blade and on the other hand with radial crossflows (radial velocity components) on fan blades of the backward skewed fan.

Concluding, it can be stated that a forward skewed fan is not always the best choice concerning aeroacoustic noise radiation. Especially under conditions with increased inflow turbulence, it can be beneficial to use a different stacking strategy – particularly backward skewed fan blades.

BIBLIOGRAPHY

- [1] S.J. Gallimore, J.J. Bolger, N.A. Cumptsy, M.J. Taylor, P.I. Wright, J.M.M. Place – *The use of sweep and dihedral in multistage axial flow compressor blading—part I: university research and methods*. ASME Journal of Turbomachinery, vol. 124, pp. 521-541, **2002**
- [2] M.G. Beiler – *Untersuchung der dreidimensionalen Strömung durch Axialventilatoren mit gekrümmten Schaufeln*. Dissertation Universität Siegen, Fortschr.-Ber. VDI Reihe 7 Nr. 298, VDI Verlag, **2002**
- [3] Y. Li, H. Ouyang, Z. Du – *Experimental research on aerodynamic performance and exit flow field of low pressure axial flow fan with circumferential skewed blades*. Journal of Hydrodynamics, vol. 19(5), pp. 579-586, **2007**

- [4] T. Carolus, M. Beiler – *Skewed blades in low pressure fans: a survey of noise reduction mechanisms*. AIAA-97-1591, pp. 47-53, **1997**
- [5] T. Wright, W.E. Simmons – *Blade sweep for low speed axial fans*. ASME Journal of Turbomachinery, vol. 112, pp. 151-158, **1990**
- [6] M. Sturm, T. Carolus – *Tonal fan noise of an isolated axial fan rotor due to inhomogeneous coherent structures at the intake*. Proceedings of FAN 2012, 18-20 April 2012, Senlis, **2012**
- [7] E.J. Kerschen, A. Envia – *Noise generation by a finite swept airfoil*. AIAA Paper 83-0768, **1983**
- [8] M. Schneider – *Der Einfluss der Zuströmbedingungen auf das breitbandige Geräusch eines Axialventilators*. Dissertation Universität Siegen, **2005**
- [9] C. Pfeleiderer, H. Petermann – *Strömungsmaschinen*. Springer, **1991**
- [10] T. Carolus – *Ventilatoren – Aerodynamischer Entwurf, Schallvorhersage, Konstruktion*. Springer Vieweg, **2013**
- [11] M. Drela – *XFOIL: An analysis and design system for low Reynolds number airfoils*. Lecture Notes in Engineering, Vol. 54, Springer **1989**
- [12] ISO 5801:2007 – *Industrial fans — Performance testing using standardized airways*. **2007**
- [13] DIN EN ISO 3744 – *Akustik – Bestimmung der Schallleistungs- und Schallenergiepegel von Geräuschquellen aus Schalldruckmessungen*. **2011**
- [14] J. Vad – *Blade sweep applied to axial fan rotors of controlled vortex design*. Dissertation Hungarian Academy of Sciences, Budapest, **2011**
- [15] A. Corsini, F. Rispoli – *Using sweep to extend the stall-free operational range in axial fan rotors*. Proceedings of the Institution of Mechanical Engineers, Part A: Journal of Power and Energy, **2004**
- [16] P.E. Roach – *The generation of nearly isotropic turbulence by means of grids*. International Journal of Heat and Fluid Flow, vol. 8(2), pp. 82-92, **1987**